THE ASTROPHYSICAL JOURNAL, 388:541–554, 1992 April 1

ENERGY DEPENDENCE OF NORMAL BRANCH QUASI-PERIODIC INTENSITY OSCILLATIONS IN LOW-MASS X-RAY BINARIES

GUY S. MILLER
Los Alamos National Laboratory, and Department of Physics and Astronomy, Northwestern University, 2145 Sheridan Road, Evanston, IL 60208
AND
FREDERICK K. LAMB
Departments of Physics and Astronomy, University of Illinois at Urbana-Champaign, 1110 W. Green Street, Urbana, IL 61801
Received 1991 May 6; accepted 1991 August 13

ABSTRACT

The properties of the ~6 Hz quasi-periodic X-ray intensity oscillations observed in the low-mass X-ray binary Cyg X-2 when it is on the normal spectral branch are shown to be consistent with a model in which photons from a central source with a fixed spectrum are Comptonized by an oscillating radial inflow. As the electron scattering optical depth of the flow varies, the spectrum of the escaping X-rays appears to rotate about a pivot energy E_p that depends mainly on the electron temperature in the flow. The temperature derived from the observed energy dependence of the Cyg X-2 normal branch oscillations is approximately 1 keV, in good agreement with the estimated Compton temperature of its X-ray spectrum. The mean optical depth τ of the Comptonizing flow is inferred to be about 10, while the change in τ over an oscillation is estimated to be about 1; both values are in good agreement with radiation hydrodcode simulations of the radial flow. The effect of induced scattering is investigated and used to place an approximate lower bound on the volume of the Comptonizing region. We conjecture that the 6 Hz normal branch oscillations observed in other Z-class sources are also produced largely by oscillations in the degree of Comptonization of a central source.

Subject headings: accretion, accretion disks — radiation mechanisms: Compton and inverse Compton — stars: neutron — X-rays: stars

1. INTRODUCTION

The X-ray intensities of many of the most luminous low-mass X-ray binaries, including Cyg X-2, Sco X-1, and GX 5-1, have been observed to vary quasi-periodically (for reviews of the observations, see Lewin, van Paradijs, & van der Klis 1988 or van der Klis 1989). These quasi-periodic oscillations (QPOs) are observed as peaks in power density spectra of the intensity time series.

The properties of the QPOs observed in the so-called Z-class low-mass X-ray binaries (LMXBs) depend on the spectral state of the source. When a harder X-ray color (for example, the count rate of photons with energies between 6 keV and 20 keV divided by the count rate between 3 and 6 keV) is plotted against a softer color (for example, the 3–6 keV count rate divided by the 1–3 keV count rate), these sources trace out all or part of a "Z"-shaped curve (see Hasinger & van der Klis 1989). Oscillations with frequencies in the range 20–50 Hz are observed when sources are on the upper branch of the Z, which is called the *horizontal branch*. The power of these *horizontal branch oscillations* (HBOs) declines as a source moves from the horizontal branch to the middle branch of the Z, which is called the *normal branch*. Oscillations of a different type, with frequencies ~5–7 Hz, appear when a source reaches the middle of the normal branch. The peak in the power spectrum associated with these *normal branch oscillations* (NBOs) broadens and shifts upward slightly in frequency as the source reaches the lower corner of the Z and begins to move up the *flaring branch*.

The Z-class LMXBs are thought to be binary systems in which a weakly magnetic neutron star accretes gas from a Keplerian disk fed by its low-mass companion. The HBOs are widely thought to be caused by interaction of the small magnetosphere of the neutron star with inhomogeneities in the inner part of the accretion disk (Alpar & Shaham 1985; Lamb et al. 1985; Shibazaki & Lamb 1987).

Recently, a radiation-hydrodynamic model of the NBOs has been proposed (Lamb 1989, 1991; Fortner, Lamb, & Miller 1989, 1991) as part of a unified model of the X-ray spectra and rapid variability of the low-mass X-ray binaries (Lamb 1989, 1991). In this model, the X-ray–emitting region has two or three important components, depending on the luminosity. The first is the central photon source, which includes the neutron star, its small magnetosphere, and the innnermost part of the accretion disk. The second component is a relatively hot ($T_e \sim$ 10–30 keV) and optically-thick compact central corona that envelopes the innermost disk and the magnetosphere. When the luminosity of the system is close to the Eddington critical luminosity L_E, plasma leaving the inner accretion disk forms the third component, an approximately radial inflow extending from an outer radius $r_o \approx 300$ km to the compact central corona at $r_c \approx 20$ km.

In the radiation-hydrodynamic model, NBOs are produced by oscillations in the optical depth of the radial inflow. Because the luminosity is close to L_E, radiation forces strongly influence the flow. To see how oscilations in the flow arise, consider as a simple example the response of the radial flow to a small increase in the density near its outer boundary. As the density enhancement is advected inward, its interaction with the X-ray flux near the inner boundary of the radial flow increases the outward flux of radiation. This increase in the radiation flux in turn increases the outward radiation force on plasma entering the radial flow, impeding its entry and producing a new density

enhancement near the flow's outer boundary. In this way the interaction between the radiation and the flow produces quasi-periodic oscillations in the flow, with a period comparable to the inflow time from the outer edge of the radial flow. As the density in the radial flow oscillates, so does its optical depth. This causes the degree of Comptonization of the radiation coming from the compact central corona to oscillate, producing a quasi-periodic oscillation in the observed X-ray spectrum.

In this paper we investigate in detail the possibility that the NBOs are due largely to quasi-periodic oscillations in the degree of Comptonization suffered by X-rays coming from a central source. We describe the Comptonization model that we use, its solution, and the resulting oscillation amplitude as a function of X-ray energy in § 2. We discuss the change in the spectrum of the escaping X-rays produced by electron thermal motions, by the convergence of the flow, and by induced scattering, when the electron-scattering optical depth of the radial flow varies. We show that the relative oscillation amplitude at sufficiently high and low photon energies can be described approximately by simple analytic expressions. In § 3 we systematically explore the sensitivity of the relative oscillation amplitude to the shape of the spectrum injected into the radial flow by the central corona and the properties of the flow. In § 4, we show how the relative oscillation amplitude can be used to determine the properties of the Comptonizing flow. The relative oscillation amplitude predicted by our model is in excellent agreement with the X-ray spectrum and relative oscillation amplitude observed in Cyg X-2. Our results and conclusions are summarized in § 5.

2. EFFECTS OF COMPTONIZATION

The analysis of oscillations of the X-ray spectrum produced by the interaction of the outflowing radiation with the oscillating radial inflow is simplified by the fact that absorption of photons by the flow is negligible. Thus, the dominant process modifying the spectrum of the X-rays escaping through the flow is Comptonization. Moreover, the mean time taken by a photon to escape from the flow is short compared to the inflow time, which is also the characteristic time scale for changes in the electron scattering optical depth of the flow. Hence, the X-ray spectrum emerging from the radial flow at a given instant can be calculated by considering only the properties of the flow at that time, and the variation of the X-ray spectrum with time during a quasi-periodic flow oscillation can be determined by computing the spectrum produced by the radial flow at successive instants during the oscillation.

Photons leaving the compact central corona enter the radial flow and scatter from the electrons there many times before escaping. The positive and negative Doppler shifts associated with the thermal motions of the electrons cause the photons to diffuse in energy. In addition, photons systematically lose energy due to the recoil of stricken electrons and gain energy from the thermal motions of the electrons. Including only these effects is adequate when a dilute photon gas interacts with a warm, static plasma. However, in the situation of interest here the inflow is converging and the photon density is high, and hence two other effects must be included in our treatment of the the Comptonization process.

First, the converging flow does work on the photon gas by compressing it. Hence, superposed on the other photon energy changes is a systematic upscattering proportional to the product of the compression rate and the mean time between collisions (Blandford & Payne 1981). Second, when the photon density is so high that the occupation number of photon states is $\gtrsim 1$, Bose statistics appreciably influence the outcomes of individual scattering events, causing the photons to bunch in the same quantum states. Although this effect is included in most derivations of the photon kinetic equation (see Rybicki & Lightman 1979; Katz 1987, p. 100), it is usually neglected in astrophysical applications. This considerably simplifies the calculation of Comptonized spectra, since the kinetic equation is then linear and hence amenable to solution by any of several methods, such as Green functions (see Sunyaev & Titarchuk 1980; Colpi 1988). In many cases the photon density is sufficiently low that this approximation is justified. However, in the model considered here, the X-ray source is extremely luminous and the Comptonization volume comparatively small. As a result, the photon density may be high enough for induced scattering to affect the spectrum. We therefore include the effects of induced scattering in our study.

2.1. *Comptonization Model*

In calculating the spectrum of the X-rays emerging from the radial flow at a given instant, we make several simplifying approximations. We model the flow by an infinite medium in which the electron and photon densities and energy distributions are uniform. The geometry of the radial flow and its finite spatial extent are incorporated into the model by specifying the distribution of photon escape times, which fixes the distribution of photon residence times in the Comptonizing region, and the density of the background photons, which is larger for smaller regions with the same photon injection rate and mean escape time. The effect of the radial flow's convergence is treated by including an appropriate term in the photon kinetic equation. This term is proportional to the compression rate of the flow ($-\nabla \cdot \boldsymbol{v}$, where $\boldsymbol{v}$ is the flow velocity) divided by the electron density. For simplicity, we assume that this ratio is independent of position, so that the effects of compression are the same everywhere.

With these assumptions, the probability $f_{\rm esc}(E)dE$ that a photon escaping from the Comptonizing region has energy between E and $E + dE$ is given by the distribution

$$f_{\rm esc}(E) = \int_0^\infty f(E, t)\,\frac{dP}{dt}\,(t)\,dt\,, \tag{2.1}$$

where $f(E, t)$ is the distribution in energy of photons that have been in the Comptonizing flow for a time t and $P(t)$ is the probability that a photon injected into the flow at time $t = 0$ escapes in a time t or less; $dP(t)/dt$ is therefore the photon escape rate at time t.

The distribution in energy $f_{\rm flow}(E)$ of all the photons present in the Comptonizing flow at a given time is the sum over ages of the distribution in energy of photons with a given age, weighted by the probability that a given photon has that age, that is,

$$f_{\rm flow}(E) = \frac{1}{\bar{t}} \int_0^\infty f(E, t)[1 - P(t)]dt\,. \tag{2.2}$$

Here

$$\bar{t} \equiv \int_0^\infty t\,\frac{dP}{dt}\,(t)\,dt \tag{2.3}$$

is the mean residence time of photons in the Comptonizing flow.

We now discuss the photon escape probability $P(t)$ and the time evolution of the photon distribution $f(E, t)$.

2.2. *Photon Escape Probability*

The probability $P(t)$ that a photon remains in the radial inflow for a time t or less before escaping depends on the structure of the flow. As a first approximation, we adopt the simple expression

$$P(t) = (1 - e^{-t/t_{\rm esc}})^2 , \tag{2.4}$$

where $t_{\rm esc}$ is the escape time. This expression resembles the probability for diffusive escape from the center of a uniform spherical scattering medium and from the center of a uniform slab. Use of a more accurate expression for $P(t)$ seems unwarranted, given our limited current understanding of the structure of the radial flow (see Lamb 1991 and Fortner, Lamb, & Miller 1989, 1991) and the other approximations inherent in our present treatment of Comptonization in the radial flow.

Expression (2.4) implies that no photons escape from the Comptonizing flow immediately, since $dP/dt = 0$ at $t = 0$. When the electron scattering optical depth of the flow is much greater than unity, expressions with this behavior are preferable to expressions which have $dP/dt \neq 0$ at $t = 0$, since expressions of the latter type grossly overestimate the number of early escapes. However, when the optical depth is less than or of order unity, expression (2.4) underestimates the number of prompt escapes. A modification of expression (2.4) that better describes escape from regions with low optical depths is given in Appendix A, although this expression is not used in the calculations we report here.

We determine the escape time by requiring that the late-time dependence of expression (2.4) agree with the late-time dependence of the exact solution to the problem of diffusive escape from a uniform spherical cloud (Sunyaev & Titarchuk 1980) of the same optical depth as the radial flow. The result is

$$t_{\rm esc} = \frac{3}{\pi^2}\left(\tau + \frac{2}{3}\right)^2 t_c , \tag{2.5}$$

where

$$\tau = \sigma_{\rm T} \int_{r_c}^{r_o} n_e(r)\, dr \tag{2.6}$$

is the scattering optical depth of the flow, and

$$t_c = (n_e c \sigma_{\rm T})^{-1} \tag{2.7}$$

is the collision time in terms of the electron density n_e, the speed of light c, and the Thomson scattering cross section $\sigma_{\rm T}$.

2.3. *Evolution of the Photon Energy Distribution*

Now consider a collection of photons injected into the Comptonizing flow at time $t = 0$ with energy distribution $f_{\rm in}(E)$. The time development of the photon energy distribution $f(E, t)$ is governed by a Kompaneets equation (see Rybicki & Lightman 1979; Katz 1987, p. 100), modified to include the upscattering produced by the converging flow (Blandford & Payne 1981). This equation may be written

$$t_c\, \partial_t f(E, t) = D[f] , \tag{2.8}$$

where

$$D[f] \equiv \partial_E\left[-\left(\frac{t_c}{t_u} + 4\frac{k_B T_e}{m_e c^2}\right)Ef + \frac{E^2}{m_e c^2} f + \frac{k_B T_e}{m_e c^2}\, \partial_E(E^2 f) + s f_{\rm flow} f\right] . \tag{2.9}$$

Equation (2.8) is a continuity equation in energy space; the terms within the brackets in the definition (2.9) of the operator D constitute the normalized photon number flux from higher to lower energies. The appropriate boundary conditions on this flux are that it vanish as $E \to 0$ and as $E \to \infty$. The systematic upscattering produced by the converging flow is described by the term $-(t_c/t_u)Ef$, where

$$t_u \equiv -3(\nabla \cdot v)^{-1} . \tag{2.10}$$

Induced scattering is described by the term $s f_{\rm flow} f$, where

$$s \equiv \frac{\dot{N}_{\rm in}\bar{t}}{V}\pi^2\frac{(\hbar c)^3}{m_e c^2} \tag{2.11}$$

in terms of the rate $\dot{N}_{\rm in}$ at which photons of all energies are injected into the Comptonizing region and the effective volume V of the region.

If, as in the radial flow, the specific heat of the electrons in the Comptonizing region is small compared to that of the photons and heating and cooling of the electrons by mechanisms other than Comptonization is negligible (Lamb 1989, 1991), the electron temperature T_e is rapidly driven to the Compton temperature

$$k_B T_c \equiv \frac{\int_0^\infty [E^2 f_{\rm flow}(E) + m_e c^2 s f_{\rm flow}^2(E)]dE}{4\int_0^\infty E f_{\rm flow}(E) dE} \tag{2.12}$$

and remains very close to this temperature during the flow oscillations.

When $T_e = T_c$, systematic upscattering of photons by the electron thermal motions and systematic downscattering due to electron recoil are in balance. Nevertheless, the photons steadily gain energy from the *bulk* motion of the converging flow, via the systematic upscattering described by the compressional term in equation (2.9). The rate at which the mean energy $\langle E\rangle = \int Ef\, dE$ of the photon distribution increases is

$$\frac{d}{dt}\langle E\rangle = \frac{1}{t_u}\langle E\rangle . \tag{2.13}$$

As a result of this increase, the mean energy $\langle E\rangle_{\rm esc}$ of the photons escaping from the Comptonizing flow is greater than the mean energy $\langle E\rangle_{\rm in}$ of the photons injected into it by a factor

$$\frac{\langle E\rangle_{\rm esc}}{\langle E\rangle_{\rm in}} = \int_0^\infty e^{t/t_u}\frac{dP}{dt}(t)dt = \frac{2t_u}{t_u - t_{\rm esc}} - \frac{2t_u}{2t_u - t_{\rm esc}} \approx 1 + \frac{3}{2}\frac{t_{\rm esc}}{t_u} . \tag{2.14}$$

Here the second equality assumes that the escape probability is given by equation (2.4) and that $t_{\rm esc} < t_u$ (*i.e.*, the photons are not trapped by the converging flow), while the final approximation is accurate when $t_{\rm esc} \ll t_u$.

In solving for the photon energy distribution $f(E, t)$, the operator D may be treated as time-independent if the compressional upscattering time t_u, photon collision time t_c, electron temperature T_e, background photon distribution $f_{\rm flow}$, and induced scattering parameter s vary only on time scales much longer than the mean time for photons to escape from the Comptonizing flow (which is $3t_{\rm esc}/2$ for the escape probability

assumed here; see eq. [2.4]). The appropriate solution to equation (2.8) is then

$$f(E, t) = e^{(t/t_c)D} f_{\rm in} , \tag{2.15}$$

where $f_{\rm in}$ is the injected spectrum.

2.4. *Differential Oscillation Amplitude*

As explained earlier, photons injected from the compact central corona into the radial flow escape in a time much smaller than the time scale of variations in the flow. We can therefore investigate the oscillation of the X-ray spectrum produced by the oscillations in the radial flow by solving the time-independent Comptonization problem for the conditions that obtain in the flow at successive instants during the oscillations and then comparing these solutions with one another.

As discussed further below, the electron scattering optical depth τ of the radial flow is expected to vary significantly during each oscillation quasi-period. Hence, in the following development we use the value of τ to specify the phase of the oscillation. In this approach, the quantities t_u, t_c, T_e, $f_{\rm flow}$, and s, which specify the conditions in the Comptonizing flow, are regarded as functions of τ.

The number of photons escaping from the Comptonizing flow per unit energy per unit time at a given phase of the oscillation is $\dot{N}_{\rm esc}(E) = \dot{N}_{\rm in} f_{\rm esc}(E)$. Suppose now that as the scattering optical depth of the flow changes by an amount $\Delta\tau$, the spectrum of the photons escaping from the flow changes by an amount $\Delta\dot{N}_{\rm esc}(E)$. Observationally, this variation appears as a change in the number of photons counted by a detector in a given range of energies ΔE during the detector integration time $t_{\rm int}$, which we assume is much smaller than the quasi-period of the oscillation. The change in the number of photons counted is

$$\Delta N(E) = \int_{\Delta E} a(E) \Delta\dot{N}_{\rm esc}(E) t_{\rm int}(E) dE , \tag{2.16}$$

where the function $a(E)$ accounts for effects such as dilution of the photon flux with the inverse square of the distance and interstellar absorption, as well as the area and quantum efficiency of the detector.

A related observable that is less sensitive to the complications represented by $a(E)$ is the *relative oscillation amplitude*

$$\gamma(E) \equiv \frac{\int_{\Delta E} a(E) \Delta\dot{N}_{\rm esc}(E) t_{\rm int}(E) dE}{\int_{\Delta E} a(E) \langle \dot{N}_{\rm esc}(E) t_{\rm int}(E) \rangle dE} , \tag{2.17}$$

where now the angle brackets indicate an average over an NBO period. If ΔE is small enough that $a(E)$, $\Delta\dot{N}_{\rm esc}(E)$, and $t_{\rm int}(E)$ vary little over the range of integration, then

$$\gamma(E) \approx \xi(E) \Delta\tau , \tag{2.18}$$

where

$$\xi(E) \equiv \frac{d}{d\tau} \ln [\dot{N}_{\rm in} f_{\rm esc}(E)] \tag{2.19}$$

is the differential relative oscillation amplitude. For conciseness, we shall henceforth refer to $\xi(E)$ simply as the *differential amplitude*. In equation (2.19),

$$f_{\rm esc} = \int_0^\infty e^{(t/t_e)D} f_{\rm in} \frac{dP}{dt}(t) dt \tag{2.20}$$

is the energy distribution of the photons escaping from the Comptonizing flow (see eqs. [2.1] and [2.15]); the Compton time t_c, photon injection spectrum $f_{\rm in}$, escape probability $P(t)$, and evolution operator D generally all vary with τ.

2.5. *Treatment of Photon Injection*

In general, the differential amplitude $\xi(E)$ will have contributions from changes in the photon flux $\dot{N}_{\rm in} f_{\rm in}(E)$ from the central corona as well as from changes in the properties of the Comptonizing flow. Unfortunately, however, the X-ray emission from the neutron star, its magnetosphere, the inner part of the accretion disk, and the compact central corona is poorly understood at present, so that a convincing calculation of the change in $\dot{N}_{\rm in} f_{\rm in}(E)$ during an oscillation of the inflow is not currently possible.

Given our lack of knowledge of the variation in $\dot{N}_{\rm in} f_{\rm in}(E)$ during an oscillation, we could allow it to vary arbitrarily during the oscillation. We would almost certainly be able to replicate the observed variation of the X-ray spectrum during the NBOs using such an approach, but the inferred variation would not be unique, the Comptonizing flow would be almost superfluous, and we would learn little or nothing of interest from the exercise.

Hence, in the calculations that follow we shall assume instead that the relative variation in $\dot{N}_{\rm in} f_{\rm in}(E)$ during NBOs can be neglected, and see how far this approximation can take us toward understanding the variation in the X-ray spectrum. In fact, this assumption is not wholly implausible. We expect photons to be produced near the neutron star by processes such as cyclotron emission and bremsstrahlung, and then to be partially Comptonized by the hot electrons in the central corona. If the relative variations in the photon production rate, electron temperature, optical depth, and other properties of the central corona during an oscillation are comparable to the relative variation in the mass flux entering the central corona, then the relative variation in $\dot{N}_{\rm in} f_{\rm in}(E)$ during NBOs will indeed be much smaller than the relative variation in $f_{\rm esc}(E)$.

If the observed variation in the X-ray spectrum during NBOs can be accurately reproduced with $\dot{N}_{\rm in} f_{\rm in}(E)$ held constant, this will suggest that the observed variation is due largely to oscillations in the properties of the Comptonizing flow outside the central corona. If, on the other hand, the observed variation in the X-ray spectrum cannot be reproduced by such a model, the radiation-hydrodynamic model of NBOs might still be valid, but changes in $\dot{N}_{\rm in} f_{\rm in}(E)$ during the oscillations would have to be included. In fact, our models with $\dot{N}_{\rm in} f_{\rm in}(E)$ held constant are remarkably successful in accounting for the available data on the variation of the X-ray spectrum during NBOs, as we discuss in § 4. These data are therefore consistent with oscillating Comptonization by the radial flow.

Assuming that the change in $\dot{N}_{\rm in} f_{\rm in}(E)$ is small during an oscillation, the differential amplitude may be written

$$\xi(E) \approx \left(\frac{d \ln [f_{\rm esc}(E)]}{d\tau} \right)_{\dot{N}_{\rm in} f_{\rm in}(E)} , \tag{2.21}$$

where we have explicitly indicated that in taking the derivative with respect to τ, $\dot{N}_{\rm in} f_{\rm in}(E)$ is to be held constant. Henceforth we shall assume that $\xi(E)$ is given by this approximation.

Consider now the spectrum $f_{\rm in}(E)$ of the photons injected into the Comptonizing radial flow by the compact central corona. Moderate-luminosity LMXBs typically have power-law spectra, exponentially cut off at energies $\sim$10–30 keV (see

White, Stella, & Parmar 1988; Schulz, Hasinger, & Trümper 1989). In the unified model (Lamb 1989; 1991), these spectra are produced by unsaturated Comptonization of photons from the neutron star, magnetosphere, and inner disk by hot electrons in the compact central corona. Unsaturated Comptonization generates a stable power-law X-ray spectrum with a spectral index ~ 1–2 for a wide range of electron temperatures and source luminosities (Katz 1976; Shapiro, Lightman, and Eardley 1976). In the unified model, the spectrum produced by the central corona of a Z source when the source is near the middle of the normal branch is expected to be similar to the spectrum of a moderate-luminosity LMXB, except that Comptonization in the central corona may have begun to saturate. Also, the spectrum is expected to be cut off at low energies by self-absorption.

As we show in § 3, the differential oscillation amplitude is relatively insensitive to the detailed shape of the spectrum produced by the central corona. Hence, in the present work we shall assume that the spectrum of the photons injected into the Comptonizing radial flow by the central corona can be described adequately by a power law truncated below the low-energy cutoff $E_{\rm low}$ and exponentially cut off at E_c, that is,

$$f_{\rm in}(E) \propto \Theta(E - E_{\rm low}) E^{-\alpha} \exp\left(-E/E_c\right), \qquad (2.22)$$

where $\Theta(E)$ is the unit step function. We shall generally consider relatively flat power laws, with indices $\alpha \sim 1$–2.

2.6. *Contributions to the Differential Amplitude*

According to the unified model, when a Z source is on the normal branch, its luminosity L is within 10% of the Eddington critical luminosity L_E (Lamb 1989, 1991). In this situation it is convenient to specify the luminosity by its relative closeness to L_E, which is described by the small parameter $\epsilon = 1 - L/L_E$.

In the radiation-hydrodynamic model of the NBOs, the change in $f_{\rm esc}(E)$ during an oscillation is due to changes in the escape time, upscattering time, induced scattering, and electron temperature as the optical depth of the radial flow oscillates. Simulations of nearly critical radial flows ($\epsilon \ll 1$) show that relatively small changes in the mass accretion rate $|\Delta \dot{M}| \approx \epsilon \dot{M} \ll \dot{M}$ produce relatively large changes in the optical depth of the flow (see, *e.g.*, Fig. 2 of Fortner, Lamb, & Miller 1989). Typically, $\Delta\tau/\tau$ is at least as large as $\Delta\epsilon/\epsilon$ (in accordance with expectations formed from studies of time-independent flows; see Miller 1990 and Park & Miller 1991).

In order to estimate the relative importance of the various effects of the Comptonizing flow in determining the oscillation amplitude, we now investigate the dependence of $t_{\rm esc}/t_c$, t_c/t_u, s, and T_e on τ.

Variation in escape time.—The integral in equation (2.20) for $f_{\rm esc}(E)$ is cut off after a time $\approx t_{\rm esc}$ by the escape rate dP/dt in the integrand. Hence, for injection spectra that are, like the spectrum (2.22), relatively flat, the change in $f_{\rm esc}(E)$ produced by the exponential operator in equation (2.20) is $\sim e^{(t_{\rm esc}/t_c)D} \sim e^{y}$ at energies $E \lesssim k_B T_e$, where $y \equiv 4(k_B T_e/m_e c^2)(t_{\rm esc}/t_c)$ is the Compton y-parameter, and $\sim \exp\left(yE/k_B T_e\right)$ at energies $E \gtrsim k_B T_e$.

The magnitude of the relative variation $\Delta \ln f_{\rm esc}$ in the X-ray spectrum produced by the variation in the escape time over an oscillation period is therefore $\gtrsim |\Delta y| \sim y\,|\Delta\tau/\tau| \gtrsim y\,|\Delta\epsilon/\epsilon|$. The relative variation in the X-ray spectrum due to this effect alone is therefore much greater than the relative change in the luminosity. In fact, variation of the escape time is usually the dominant cause of the variation in the X-ray spectrum.

Variation in upscattering by the converging flow.—The dependence of t_c/t_u on the optical depth τ of the Comptonizing flow can be estimated in two different ways, which (necessarily) lead to the same result. As a first approach, recall that $t_u \approx r/v$, where v is the inward radial velocity. In order to determine the behavior of v, use the continuity equation and the results of radiation-hydrocode simulations of nearly critical radial flows (Fortner, Lamb, & Miller 1989, 1991), which show that the radial mass flux remains nearly constant during the flow oscillations (the relative change in the mass flux is found to be $\lesssim |\Delta\epsilon| \lesssim \epsilon$). Thus, the inward radial velocity is $v \approx 1/n_e r^2$ and hence $t_u \propto n_e r^3$. Now $t_c \propto 1/n_e$, and hence we conclude that $t_c/t_u \propto 1/n_e^2 r^3 \propto 1/\tau^2$.

As a second approach, consider the compressional work done on the escaping photons by the radial inflow. This work is proportional to the mass flux in the radial flow, which is expected to be a fraction $\alpha_r \lesssim 0.2$ of the total mass flux (Fortner, Lamb, & Miller 1989, 1991), and increases the mean energy of the escaping photons by a factor $\approx 1/(1 - \alpha_r)$. However, in the flow model being considered, only about half of this increase occurs outside the compact central corona, which has a radius $r_c \approx 2R$, where R is the radius of the neutron star; the other half occurs inside the central corona. Thus, the work done by the flow in the Comptonizing region being considered here increases the mean energy of the escaping photons by a factor $\langle E\rangle_{\rm esc}/\langle E\rangle_{\rm in} \approx 1/(1 - 0.5\alpha_r) \approx 1 + 0.5\alpha_r$. This increase remains approximately constant during the oscillations, since—as noted above—the radial mass flux remains nearly constant. Comparing this result with expression (2.14), we conclude that $t_{\rm esc}/t_u \approx \alpha_r/3$, independent of τ. If now $\tau \gg 1$, equation (2.5) implies

$$\frac{t_c}{t_u} \approx \left(\frac{\pi}{3}\right)^2 \frac{\alpha_r}{\tau^2} \approx \frac{0.2}{\tau^2}. \qquad (2.23)$$

In writing the second equality we have assumed $\alpha_r \approx 0.2$.

Variation in the electron temperature.—The dependence of the electron temperature T_e on the optical depth τ of the Comptomizing flow is more difficult to estimate than the dependence of the compression rate on τ, since T_e reflects changes in the energy distribution $f_{\rm flow}$ of the photons within the flow (see eq. [2.12]). Nevertheless, we can estimate simply the change in the Compton temperature T_c (and hence the change in T_e, which closely tracks T_c) when $y \ll 1$ or $y \gg 1$. These estimates show that the change in T_c is small in both these regimes.

The Compton temperature T_c is a functional of $f_{\rm flow}$, which in turn is determined largely by the value of y. From the definition (2.12) of the Compton temperature we expect $\Delta \ln T_c \lesssim \Delta \ln f_{\rm flow}$, where $\Delta \ln f_{\rm flow}$ is evaluated at an energy near $k_B T_e$. Using the chain rule, we can write

$$\Delta \ln f_{\rm flow} \approx \left(\frac{\partial \ln f_{\rm flow}}{\partial \ln T_e}\frac{d \ln T_c}{d\tau} + \frac{\partial \ln f_{\rm flow}}{\partial \tau}\right)\Delta\tau, \qquad (2.24)$$

where we have used the fact that T_e closely tracks T_c to set the total derivative of T_e with respect to the optical depth equal to the total derivative of T_c with respect to the optical depth.

Now the changes in $f_{\rm flow}$ with respect to T_e and τ are, like the changes in $f_{\rm esc}$, caused largely by the change in y. Therefore $(\partial \ln f_{\rm flow}/\partial \ln T_e) \sim y$ and $\partial \ln f_{\rm flow}/\partial\tau \sim y/\tau$ for energies near

$k_B T_e$. Equation (2.24) therefore implies

$$\Delta \ln f_{\rm flow} \sim \left(\frac{d \ln T_c}{d\tau} + \frac{1}{\tau}\right) y \, \Delta\tau \, . \tag{2.25}$$

This expression shows that if y is small, the relative change in $f_{\rm flow}$, and hence in T_c, caused by the change in τ is also small. Thus, the change in the observed spectrum is due primarily to the change in y with T_e held constant, *i.e.*, to the change in τ. If on the other hand y is large, the relative change in $f_{\rm flow}$ is again small, because the Comptonization process has saturated, producing a thermal equilibrium spectrum. Expression (2.25) then confirms that the relative change in T_c, and hence in T_e, is small, and that the change in the observed spectrum is again due primarily to the change in y with T_e held constant. We therefore expect only a small change in T_e during the flow oscillations.

In § 3, we show by numerical solution of the Kompaneets equation that the differential amplitude that results when T_e is allowed to follow the Compton temperature T_c as τ varies is very similar to the differential amplitude that results when T_e is held fixed, for the physical conditions that we consider. Therefore, although we could in principle solve for the change in T_e with τ, in practice we shall usually neglect it.

Variation in the effects of induced scattering.—The term in the operator D that describes the effects of induced scattering is proportional to the photon distribution $f_{\rm flow}$ in the Comptonizing flow and the induced scattering strength s. The induced scattering strength s is proportional to the photon density in the Comptonizing medium and we therefore expect $s \propto \tau$. We estimate

$$s \approx 3 \times 10^{-9} (m_e c^2)^2 \tau \left(\frac{L}{10^{38}\ {\rm erg\ s^{-1}}}\right)\left(\frac{\langle E \rangle}{1\ {\rm keV}}\right)^{-1}\left(\frac{r_{\rm Compt}}{5 \times 10^6\ {\rm cm}}\right)^{-2} , \tag{2.26}$$

where $r_{\rm Compt} = (3V/4\pi)^{1/3}$ is the effective radius of the Comptonizing region.

It is difficult to determine the induced scattering strength accurately, due mainly to lack of knowledge of $r_{\rm Compt}$. The effective radius of the Comptonizing region cannot be smaller than the radius $r_c (\approx 2 \times 10^6$ km) of the compact central corona. From expression (2.26), we therefore conclude that

$$s \lesssim 10^{-8} \, (m_e c^2)^2 \tau \, . \tag{2.27}$$

The induced scattering strength will be close to this upper bound if the effective radius of the Comptonizing region is only slightly larger than the radius r_c of the compact central corona, as will be true if most of the optical depth in the radial flow is at small radii.

2.7. *Limiting Forms of the Differential Amplitude*

When the degree of Comptonization is modest, we can obtain approximate analytical expressions for the differential amplitude $\xi(E)$ at low and high photon energies. These approximations are helpful in developing intuition about the oscillation amplitude and in interpreting our numerical solutions. We therefore introduce them before describing the numerical method that we use to solve for $f_{\rm esc}(E)$ and $f_{\rm flow}(E)$.

Differential amplitude at low photon energies.—Assume that $P(t)$ is given by equation (2.4). Then the formal solution of equation (2.20) is

$$f_{\rm esc}(E) = \left[\frac{2}{1 - (t_{\rm esc}/t_c)D} - \frac{2}{2 - (t_{\rm esc}/t_c)D}\right] f_{\rm in}(E) \, . \tag{2.28}$$

For relatively flat photon injection spectra, like those described by expression (2.22), $(t_{\rm esc}/t_c)D$ is $\sim \max(y, yE/k_B T_e)$. Thus, if $y \ll 1$ and $E \ll k_B T_e/y$, the right side of equation (2.20) may be expanded in powers of $(t_{\rm esc}/t_c)D$, with the result

$$f_{\rm esc}(E) \approx [1 + \tfrac{3}{2}(t_{\rm esc}/t_c)D] f_{\rm in}(E) \, . \tag{2.29}$$

In this lowest order approximation, $f_{\rm flow}$ in the operator D may be replaced by $f_{\rm in}$.

Expression (2.29) is useful for estimating the oscillation amplitude and for assessing the importance of compressional upscattering and induced scattering at low photon energies. When the latter two effects are weak, the operator D describes the flow of photons with energies $E \gg k_B T_e$ toward lower energies and the flow of photons with energies $E \ll k_B T_e$ toward higher energies. Thus, the operator in square brackets in equation (2.29) "squeezes" a flat injected spectrum toward a peaked thermal distribution. As a result, the differential oscillation amplitude $\xi(E)$ is negative at high energies, positive at the intermediate energies toward which photons flow to form the thermal peak, and negative at low energies. The differential amplitude therefore has two nodes, one on each side of the nascent thermal peak. At energies $E \ll k_B T_e$, $(t_{\rm esc}/t_c)D \sim y$ and hence

$$\xi(E) \sim \frac{y}{\tau} \propto T_e \tau \, . \tag{2.30}$$

Thus, in this energy range the differential amplitude increases with increasing τ.

Induced scattering tends to pull photons toward energies where the photon quantum occupation number is high. If induced scattering is strong enough, photons will collect in a secondary peak near the low-energy cutoff as well as in the thermal peak, producing an additional node in $\xi(E)$ at an energy just above $E_{\rm low}$.

Differential amplitude at high photon energies.—The approximation (2.29) for $f_{\rm esc}$ relies on the fact that when $y \lesssim 1$, Comptonization has a relatively mild effect on the spectrum at low energies. As a result, the low-energy spectrum of the escaping photons differs only slightly from the low-energy spectrum of the injected photons. The effect of Comptonization on the spectrum at higher energies is much greater, and hence a different approach is required to develop an approximate solution.

At energies $E \gg k_B T_e$, the change in the photon distribution function is due largely to the effects of electron recoil; thermal broadening and upscattering proceed two slowly to have much effect on the spectrum. If electron recoil were the only process changing the photon energy distribution, the distribution would be

$$f(E, t) \approx \left(\frac{E_0}{E}\right)^2 f_{\rm in}(E_0) \, , \tag{2.31}$$

at $t < t_c (m_e c^2/E)$ and zero at later times (see, *e.g.*, Sunyaev & Titarchuk 1980). Here

$$E_0 = \left[\frac{1}{E} - \frac{1}{m_e c^2}\left(\frac{t}{t_c}\right)\right]^{-1} . \tag{2.32}$$

In reality, $f(E, t)$ is very small ($\sim \exp[-E/k_B T_e]$) but nonzero

even at late times, due to the upward diffusion of photons from low energies (see Appendix B). Expression (2.31) shows that when electron recoil is the dominant effect and we are concerned only with energies that are large compared to both $m_e c^2 t_c/t_{esc}$ and $k_B T_e$, the integral (2.1) for the energy distribution of the escaping photons is dominated by contributions from times $0 \le t \le t_c(m_e c^2/E) \ll t_{esc}$. We may therefore approximate $P(t)$ in the integrand by expanding it in powers of t/t_{esc}.

Whenever unscattered photons make a negligible contribution to the radiation flux leaving the Comptonizing flow, we may use an escape probability that satisfies $[dP/dt]_{t=0} = 0$. For any such escape probability, the first nonvanishing term in an expansion in powers of t is

$$f_{esc}(E) \approx \frac{d^2P}{dt^2}\bigg|_{t=0} \int_0^\infty f(E, t) t\, dt \propto \left(\frac{t_c}{t_{esc}}\right)^2 . \tag{2.33}$$

The resulting differential amplitude at high energies is

$$\xi(E) = -\frac{d}{d\tau} \ln\left(\frac{t_{esc}}{t_c}\right)^2 \approx -\frac{4}{\tau}, \tag{2.34}$$

which is negative and independent of energy. More importantly, it is independent of the injected spectrum. In § 3 we display differential amplitudes computed numerically for a variety of input spectra; all flatten toward the limit (2.34) at high photon energies.

2.8. *Numerical Computation of Photon Distributions*

To determine the differential amplitude for arbitrary photon energies and degrees of Comptonization, we first solve equation (2.1) for $f_{esc}(E)$ and then compute $d \ln [f_{esc}(E)]/d\tau$ numerically.

Suppose first that induced scattering can be neglected. It is convenient to introduce the family of functions

$$f_\beta(E) \equiv \frac{\beta}{t_c} \int_0^\infty f(E, t) e^{-\beta(t/t_c)}\, dt , \tag{2.35}$$

where β is a constant. If the escape probability is given by equation (2.4), then

$$f_{esc}(E) = 2f_{\beta_{esc}}(E) - f_{2\beta_{esc}}(E) , \tag{2.36}$$

where

$$\beta_{esc} \equiv t_c/t_{esc} . \tag{2.37}$$

The functions $f_\beta(E)$ satisfy the linear ordinary differential equation

$$D[f_\beta] = \beta(f_\beta - f_{in}) . \tag{2.38}$$

Thus, calculation of f_{esc} requires the solution of two linear ordinary differential equations, one for $f_{\beta_{esc}}$ and one for $f_{2\beta_{esc}}$. We solve these equations numerically using multiple shooting, a method that is well suited to stiff equations of this kind, since the integration of the equation is performed piecewise over many small intervals. Multiple shooting is the straightforward extension of the technique of shooting to an intermediate point (see Press *et al.* 1986, p. 586) to the case of multiple intermediate points.

Now suppose induced scattering is important. The operator D now depends on the distribution f_{flow} of the photons in the Comptonizing flow. We therefore solve for f_{esc} by iteration. We first assume $f_{flow} = f_{in}$ and use this estimate of f_{flow} to obtain an initial expression for D. Next, we use this expression for D to obtain approximate solutions for the auxiliary functions f_β and $f_{2\beta}$. We then use these functions to generate an improved estimate for f_{flow}, using the expression (compare eq. [2.36])

$$f_{flow}(E) = \tfrac{4}{3} f_{\beta_{esc}}(E) - \tfrac{1}{3} f_{2\beta_{esc}}(E) . \tag{2.39}$$

Finally, this estimate of f_{flow} is used to generate an improved estimate of D, and the procedure is iterated until f_{flow} and D converge.

3. DEPENDENCES OF THE OSCILLATION AMPLITUDE

In this section we investigate the dependence of the oscillation amplitude on the spectrum of the injected photons, on the mean optical depth, temperature, and volume of the Comptonizing radial flow, and on the upscattering caused by the convergence of the flow. We do this by computing the finite relative oscillation amplitude

$$\xi_f(E) \equiv 2\left[\frac{f_{esc}(E, \tau) - f_{esc}(E, \tau - 1)}{f_{esc}(E, \tau) + f_{esc}(E, \tau - 1)}\right] \tag{3.1}$$

for different injection spectra and different properties of the Comptonizing flow. Henceforth, for conciseness we shall refer to $\xi_f(E)$ simply as the *finite amplitude.*

In investigating the dependence of the finite amplitude on the shape of the injected spectrum and the properties of the Comptonizing flow, we generally choose parameter values that are characteristic of Cyg X-2, one of the best studied Z sources. Thus, except when we are exploring the effects of variations in the electron temperature T_e, we set T_e equal to 1 keV, the apparent Compton temperature of the Cyg X-2 X-ray spectrum (see § 4). Similarly, except when we are studying the dependence of the finite amplitude on the mean optical depth τ of the Comptonizing flow, we set $\tau = 10$, which is close to the mean optical depth indicated by the unified model (Lamb 1989, 1991; Fortner, Lamb, & Miller 1989, 1991). For these "standard" choices of T_e and τ, the injected spectrum is moderately Comptonized ($y = 0.27$). Finally, we neglect the effects of induced scattering and compression-driven upscattering, except when we explicitly investigate them.

3.1. *Dependence on the Injected Spectrum*

The form (2.22) that we have adopted for the injected photon spectrum $f_{in}(E)$ depends on three parameters: the spectral index α, the exponential cutoff energy E_c, and the energy E_{low} below which the spectrum is truncated. Consider first the dependence of the finite amplitude on α and E_c, for E_{low} fixed at 0.1 keV. Figure 1 shows the relative amplitude for two choices of the spectral index ($\alpha = 1.0, 1.5$) and two choices of the exponential cutoff energy ($E_c = 5$ keV, 10 keV). The most prominent feature in the relative amplitude is the node at the energy E_p, which we define as the highest energy root of $\xi_f(E)$. This node arises from the tendency of the X-ray spectrum to rotate locally about the pivot energy E_p as the optical depth of the Comptonizing flow varies, as shown in Figure 2. The finite amplitude at low energies ($E \lesssim 2$ keV) is smaller when the injected spectrum is flatter.

The pivot energy is determined by competition between the downscattering of high-energy photons described by equation (2.31) and the diffusion of photons described by equation (2.29). Although the rate of downscattering generally depends on the shape of the injected spectrum at high energies, it is fairly insensitive to E_c for moderate values of y (recall that $y \approx 0.3$ for

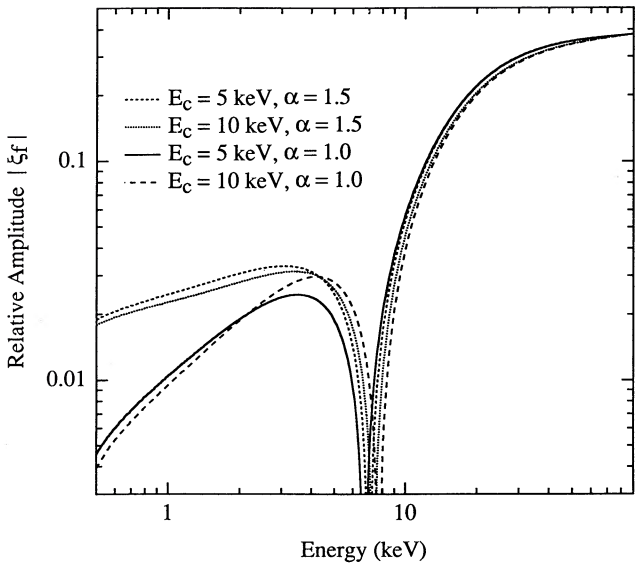

FIG. 1.—Absolute magnitude of the finite oscillation amplitudes produced by four different photon injection spectra $f_{in}(E)$, showing the node at the spectrum pivot energy $E_p \approx 7$ keV and the insensitivity of the oscillation amplitude to the shape of the injection spectrum. The injected spectra were power laws with spectral indices $\alpha = 1.0$ and 1.5 and exponential cutoff energies $E_c = 5$ and 10 keV; all four were truncated below 0.1 keV. The electron temperature in the Comptonizing region was fixed at 1 keV, while the mean optical depth of the region was fixed at 10; induced scattering and upscattering by the converging flow were both neglected. The oscillation amplitude depends on α only at low energies and is almost independent of E_c.

the electron temperature and mean optical depth assumed here). The rate of upward diffusion also depends on the shape of the injected spectrum, but at moderate energies it is insensitive to the power-law index α. The pivot energy is therefore more sensitive to E_c than to α, but depends only weakly even on E_c, increasing slightly as E_c increases from 5 to 10 keV.

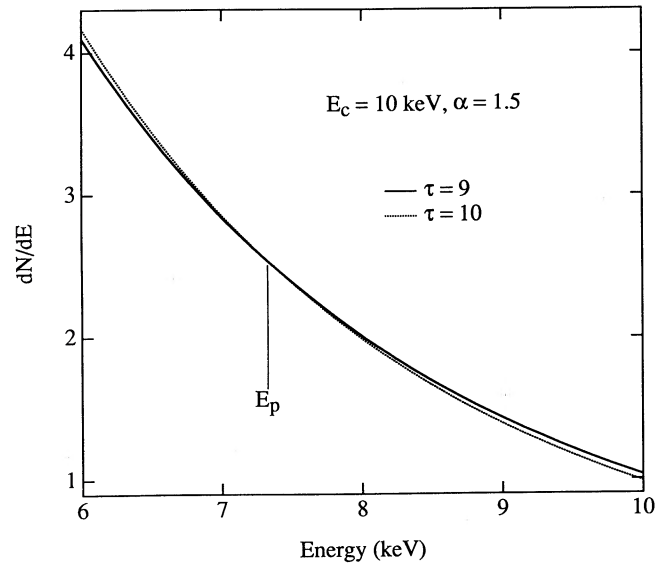

FIG. 2.—Photon number spectra for two slightly different optical depths ~ 10, illustrating the apparent rotation of the spectrum about the pivot energy E_p when the optical depth of the Comptonizing region varies. Other properties of the Comptonizing region are the same as in Fig. 1. The two spectra correspond to two different phases in the oscillation of the radial flow.

The dependence of the finite amplitude on the low-energy cutoff of the injected spectrum is illustrated in Figure 3. Here and in the remainder of this section we consider injected spectra with $\alpha = 1.5$ and $E_c = 10$ keV. As the photon distribution evolves toward its asymptotic form (see Appendix B), photons with energies just above E_{low} diffuse to energies below E_{low}. Hence $\xi_f(E)$ is negative at energies just above E_{low}. Since $\xi_f(E)$ is positive at energies $\sim T_e$, this implies that $\xi_f(E)$ has a node at an energy between E_{low} and T_e. Increasing E_{low} moves this node upward in energy. For the electron temperature and mean optical depth assumed in Figure 3, Comptonization is moderate and hence the value of E_{low} has a significant effect on $\xi_f(E)$ only when E_{low} is relatively high (~ 0.5 keV) and then only at low energies ($\lesssim 2$ keV, for the injected spectra considered). Throughout the rest of this section we therefore consider only injected spectra with $E_{low} = 0.1$ keV.

3.2. *Dependence on the Properties of the Comptonizing Flow*

The main difference between the finite amplitudes produced by Comptonizing flows with different mean optical depths is the relative size of the NBO amplitude at high and low energies, as shown by Figure 4. The relative amplitude at high energies becomes somewhat smaller with increasing τ, in accordance with equation (2.34), whereas the relative amplitude at low and moderate energies increases, in accordance with equation (2.30). The pivot energy E_p decreases with increasing τ, although not dramatically.

The pivot energy is much more sensitive to the electron temperature than to the mean optical depth, as Figure 5 makes clear. As noted earlier, the competition between diffusion due to the thermal motions of the electrons and downscattering due to electron recoil is the most important determinant of E_p. Hence, higher electron temperatures produce higher pivot

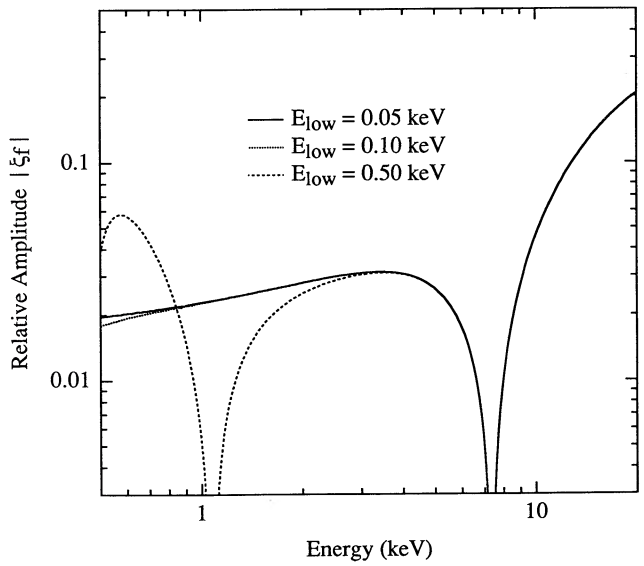

FIG. 3.—Finite oscillation amplitudes for three values of the energy E_{low} below which the spectrum of injected photons is truncated, illustrating the weak dependence on E_{low}, except when E_{low} is $\gtrsim 0.5$ keV. All three injected spectra have $\alpha = 1.5$ and $E_c = 10$ keV; the properties of the Comptonizing region are the same as in Fig. 1. When Comptonization of the injected spectrum is moderate ($y \lesssim 1$), diffusion of photons downward in energy from E_{low} creates a node in the oscillation amplitude just above E_{low} (see text). This node does not significantly affect the oscillation amplitude above 1 keV unless the truncation energy of the injected spectrum is $\gtrsim 0.5$ keV.

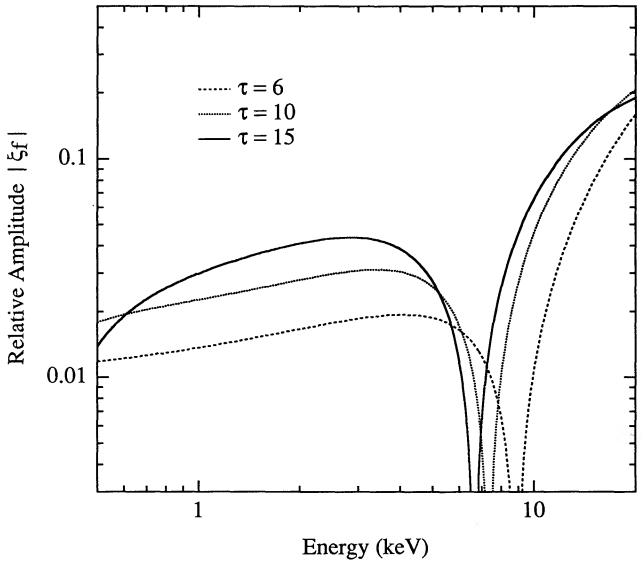

FIG. 4.—Finite oscillation amplitudes produced by Comptonizing flows with different mean optical depths, illustrating the weak dependence of the pivot energy on the optical depth of the flow. Other properties of the Comptonizing flows are the same as in Fig. 1. The truncation energy, spectral index, and exponential cutoff energy of the injected spectrum are 0.1 keV, 1.5, and 10 keV, respectively. The oscillation amplitude at high energies decreases slightly as τ increases, whereas the amplitude at low and moderate energies increases significantly.

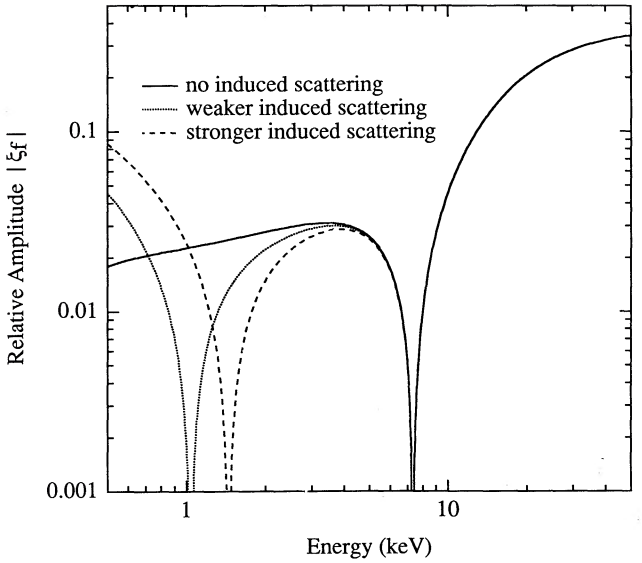

FIG. 6.—Finite oscillation amplitudes for three induced scattering strengths, showing the additional node that appears in the amplitude at low energies when induced scattering is moderately strong. The value of the induced scattering strength s is zero for the case without induced scattering, $10^{-9}[m_e c^2]^2\tau$ for the weaker-induced-scattering case, and $3 \times 10^{-9}[m_e c^2]^2\tau$ for the stronger-induced-scattering case. Other properties of the flow are the same as in Fig. 1, while the injected spectrum is the same as in Fig. 4. The effect of induced scattering is greater at lower energies because the photon mode occupation numbers are larger there.

energies. The sensitive dependence of the pivot energy on the electron temperature makes the pivot energy a good diagnostic of the electron temperature in the Comptonizing flow.

The effect of induced scattering on the finite amplitude is illustrated by the three amplitudes plotted in Figure 6. These amplitudes correspond to no induced scattering ($s = 0$), a moderate amount of induced scattering ($s = 10^{-9}(m_e c^2)^2\tau$), and a large amount of induced scattering ($s = 3 \times 10^{-9}(m_e c^2)^2\tau$). For moderately Comptonizing flows, $f_{\rm flow}(E)$ is similar to $f_{\rm in}(E)$ and falls with increasing energy for the injected spectra that we consider here. For such $f_{\rm flow}(E)$, induced scattering tends to pull photons toward low energies, where the photon mode occupation numbers are high, but inhibits the flow of photons to energies below the truncation energy $E_{\rm low}$ of the injected spectrum. This creates a peak in the spectrum of the escaping X-rays just above $E_{\rm low}$ and a node in the finite amplitude (in addition to the nodes associated with the nascent Wien maximum) just above the peak. The node immediately below E_p in energy is forced closer to E_p, since the loss of photons at low energies from thermal upscattering into the incipient Wien peak is augmented by the induced motion of photons toward the low-energy cutoff. A high truncation energy can also have this effect (see Fig. 3) since photons drain by diffusion to energies below $E_{\rm low}$, but does not produce a peak in the X-ray spectrum just above $E_{\rm low}$. Thus, if the low-energy portion of the spectrum could be observed, it would be simple to distinguish between a second node produced by the low-energy turnover of the injected spectrum (which we have modeled by truncating the spectrum at $E_{\rm low}$) and a second node produced by relatively strong induced scattering.

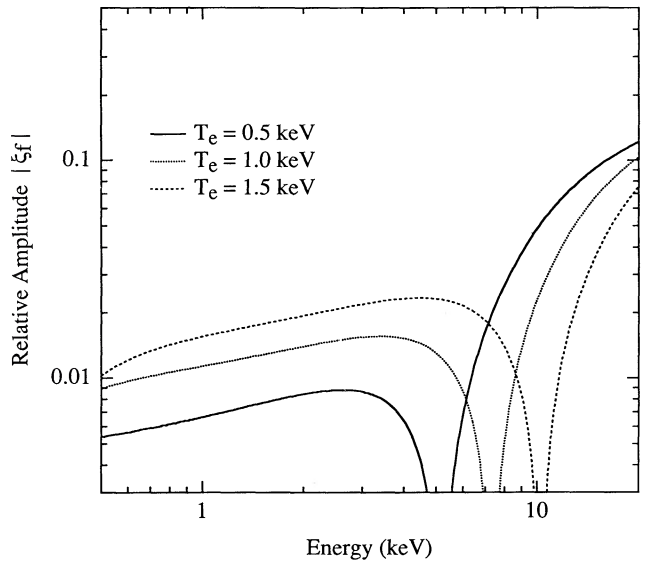

FIG. 5.—Finite oscillation amplitudes for three values of the electron temperature T_e in the Comptonizing flow, illustrating the sensitive dependence of the pivot energy on T_e. Other properties of the flow are the same as in Fig. 1 while the injected spectrum is the same as in Fig. 4. The sensitive dependence of the pivot energy on T_e makes E_p a good diagnostic of the electron temperature in the Comptonizing flow.

Although it is possible in principle to estimate the volume of the Comptonizing flow by measuring the X-ray spectrum and the relative NBO amplitude at low energies, in practice interstellar absorption at energies below ~ 1 keV is so great for the distant Z sources that such data will probably be difficult or impossible to obtain in the foreseeable future. We must therefore content ourselves with placing limits on the volume of the Comptonizing flow using data at higher energies (see § 4).

Consider now the effect of upscattering by the converging flow on the finite amplitude. Figure 7 compares finite amplitudes computed with and without this upscattering, for

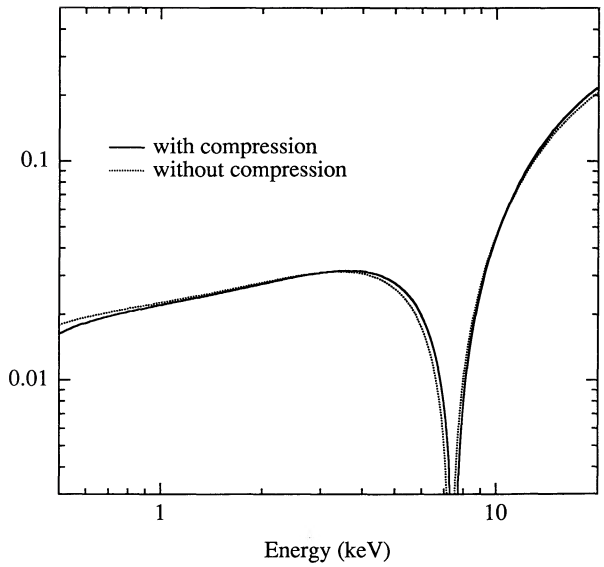

FIG. 7.—Finite oscillation amplitudes computed with and without upscattering by the converging flow, illustrating the small effect of this upscattering for the flow model assumed here. For the case with compressional upscattering, $t_c/t_u = 0.2/\tau^2$. Other properties of the flow are the same as in Fig. 1, while the injected spectrum is the same as in Fig. 4. Because the rate of compressional upscattering is $\propto t_{esc}/t_u$, it is independent of the optical depth of the flow. The X-ray spectrum therefore changes little as the optical depth of the flow oscillates, leaving the oscillation amplitude almost unaffected by the upscattering.

Comptonizing regions that are otherwise the same and injected spectra that are identical. In general, although upscattering by the converging flow changes the X-ray spectrum, it has little effect on the relative amplitude. The reason is that in the flow model considered here, the rate of this upscattering is $\propto (t_{esc}/t_c)(t_c/t_u)$ and is therefore independent of the optical depth of the flow. As a result, the spectrum of the escaping radiation is nearly fully modified by interaction with the converging flow even when the optical depth is small. The X-ray spectrum therefore changes little as the optical depth of the flow oscillates, leaving the finite amplitude almost unaffected by the upscattering.

Finally, we investigate the effect on the finite amplitude of the slight oscillation in the Compton temperature T_c of the radiation within the radial flow that occurs as the optical depth of the flow oscillates. For example, if the injected spectrum has $E_{low} = 0.1$ keV, $\alpha = 1.5$, and $E_c = 10$ keV, T_c decreases from 1.07 keV to 1.03 keV as τ increases from 9 to 10. The oscillation in T_c causes the electron temperature in the flow to oscillate by a small amount. Figure 8 compares the finite amplitude obtained when the electron temperature in the flow is allowed to follow oscillations in the Compton temperature with the amplitude obtained when the electron temperature is kept fixed at 1.05 keV. The differences between the two amplitudes are small.

4. APPLICATION TO NORMAL BRANCH OSCILLATIONS

In the unified model of X-ray emission from neutron stars in LMXBs, X-ray photons coming from the neutron star, its small magnetosphere, and the innermost part of the accretion disk are Comptonized by a small, relatively hot central corona that envelopes the inner disk and magnetosphere (Lamb 1989, 1991), producing the horizontal branch spectra of the Z sources. When the luminosity approaches the Eddington critical luminosity, the radiation coming from the central corona is further Comptonized by a cool, approximately radial inflow from the inner disk (Lamb 1989, 1991; Fortner, Lamb, & Miller 1989, 1991), producing the normal branch spectra of the Z sources.

Detailed computations of radiative transfer through static scattering envelopes have shown that Comptonization models can accurately reproduce the observed X-ray spectra of a variety of LMXBs, when the spectrum of the central photon sources is treated as adjustable (see, *e.g.*, Ponman, Foster, & Ross 1990). Although such models provide valuable information about physical conditions in the outer Comptonizing region, their success and the physical conditions inferred from them depend on the spectrum assumed for the radiation coming from the central source. Our lack of knowledge concerning this spectrum is therefore a major source of uncertainty in these models.

The results presented in the previous section show that the relative change in the X-ray spectrum that occurs when the optical depth of the Comptonizing flow changes by a small amount is fairly insensitive to the spectrum assumed for the radiation coming from the central source, at least if that spectrum is qualitatively similar to the spectra observed in LMXBs and the properties of the Comptonizing flow are similar to those expected in the unified model. On the other hand, the relative change in the X-ray spectrum is fairly sensitive to the properties of the Comptonizing flow. This has two important implications. First, we can test the hypothesis that the NBOs are caused largely by oscillations in the optical depth of a Comptonizing flow, even though we do not yet have a detailed physical model of the central radiation source. Second, if the hypothesis that the NBOs are produced largely by oscillations in the degree of Comptonization is successful, we can infer the properties of the Comptonizing flow with relatively high confidence.

Suppose that the oscillating Comptonization model is able

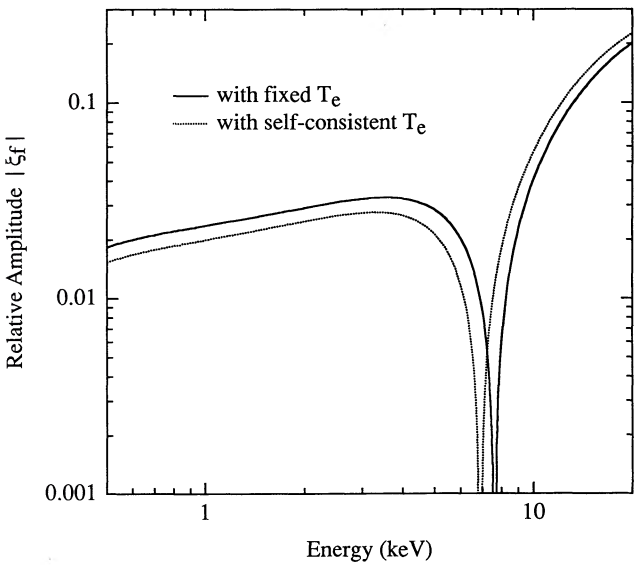

FIG. 8.—Finite oscillation amplitudes obtained when the electron temperature in the Comptomizing flow is allowed to adjust to the Compton temperature and when the electron temperature is kept fixed, showing that the differences between the two amplitudes are small. Other properties of the flow are the same as in Fig. 1, while the injected spectrum is the same as in Fig. 4.

to adequately describe the observed relative oscillation amplitude $\gamma_{obs}(E)$ with the spectrum of the central source held fixed. Then the results of § 3 show that three important properties of the Comptonizing flow can be immediately read off from the properties of $\gamma_{obs}(E)$. First, the relative change in the optical depth of the Comptonizing flow, $\Delta\tau/\tau$, is fixed by the magnitude of $\gamma_{obs}(E)$ at high energies (see eqs. [2.18] and [2.34]). Second, the temperature T_e of the electrons in the Comptonizing flow is determined by the position of the highest-energy node in $\gamma_{obs}(E)$, which coincides with the spectrum pivot energy E_p and is sensitive to T_e. Third, the magnitude of $\gamma_{obs}(E)$ at energies below E_p depends primarily on Δy, which is proportional to $T_e\tau\Delta\tau$ (see eqs. [2.18] and [2.30]). Hence, from measurements of $\gamma_{obs}(E)$ we can in principle determine (1) the mean optical depth τ of the Comptonizing flow, (2) the variation $\Delta\tau$ of the optical depth during the NBO, and (3) the electron temperature T_e in the Comptonizing flow. With these parameters determined, the validity of the oscillating Comptonization model can be checked by a detailed comparison of the relative NBO amplitude $\gamma(E)$ predicted by the model with $\gamma_{obs}(E)$.

A further test of the model can be made if one compares the electron temperature T_e inferred by fitting $\gamma(E)$ to $\gamma_{obs}(E)$ with the Compton temperature T_c' obtained from approximating the photon spectrum $f_{flow}(E)$ within the Comptonizing flow by the observed photon spectrum $f_{obs}(E)$ and using expression (2.12). The agreement between the inferred electron temperature and T_c' may not be exact, since this approximation neglects the difference between $f_{flow}(E)$ and $f_{obs}(E) = f_{esc}(E)$. Also, for most Z sources few measurements of the spectrum in the soft X-ray band are available and the amount of interstellar absorption is uncertain. Thus some assumptions about the spectrum of the source below 2 keV are necessary in order to compute T_c' (although T_c' is not particularly sensitive to the spectrum below 1 keV). Nevertheless, a gross discrepancy between T_e and T_c' would be a problem for the model.

We now apply the procedure just described to observations of Cyg X-2, one of the best-studied Z sources. Figure 9 shows the relative amplitude of the Cyg X-2 NBO in the energy range 1–19 keV as measured by Mitsuda (1988) using the *Ginga* satellite. The horizontal bars indicate the energy bins used in plotting the data. The crosses show the rms variation in the number of counts in each energy bin divided by the mean number of counts during a sequence of 8 ms integration times. The vertical bars indicate 90% confidence intervals. The counts in the highest and lowest energy bins are thought to be dominated respectively by the lowest and highest energy photons within these bins, because the detector response increases rapidly with energy in the lowest bin and falls rapidly with energy in the highest bin.

Also shown in Figure 9 is the relative variation in the number of counts predicted by the oscillating Comptonization model with $T_e = 1.0$ keV, $\tau = 10$, and $\Delta\tau = 0.9$. The basis for these parameter choices is described below. The injected spectrum is of the form (2.22) with $E_{low} = 0.1$ keV, $\alpha = 1.5$, and $E_c = 10$ keV. This injected spectrum is similar to the spectra observed in lower luminosity LMXBs and thought to arise in the compact central corona expected in the unified model (see § 2). The Compton temperature of the injected spectrum is ≈ 1 keV.

We now discuss the constraints on the Comptonizing flow parameters implied by the Cyg X-2 countrate variations shown in Figure 9. Although the amount of interstellar absorption

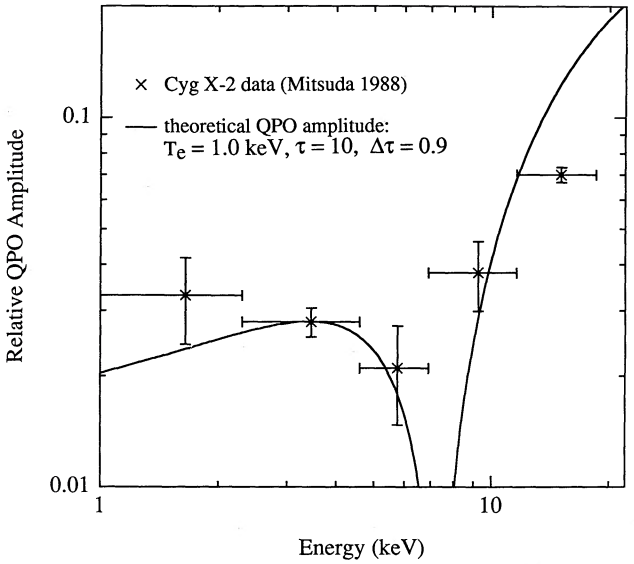

FIG. 9.—Comparison of the relative NBO amplitude in Cyg X-2 observed by Mitsuda (1988) with the relative NBO amplitude predicted by the oscillating Comptonization model. The oscillating flow has $T_e = 1.0$ keV, $\tau = 10$, and $\Delta\tau = 0.9$, and the injected spectrum is the same as in Fig. 4. The horizontal bars indicate the energy bins used in plotting the data. The crosses show the rms variation in the number of counts in each energy bin divided by the mean number of counts during a sequence of 8 ms integrations. The vertical bars indicate 90% confidence intervals. The predicted variation is in excellent agreement with the observed variation.

and the response of the detector do not affect the relative NBO amplitude at a given energy, they *do* affect the averaging that must be done to predict the relative countrate variation that will be observed in energy bins of finite width. We have not taken these effects into account. Moreover, our model of the Comptonizing radial flow is highly simplified. Therefore, we confine ourselves to conclusions that follow from comparing the qualitative features of the countrate variations predicted by the model with the observed countrate variations.

Even with these qualifications, the countrate variations observed in Cyg X-2 place remarkably narrow limits on the properties of the Comptonizing radial flow. Consider first the electron temperature. Figure 9 shows that the relative countrate variation is lowest near 6 keV. Other data indicate that the phase of the variation changes by $\sim 180°$ in the energy range 4.5–8 keV (see Mitsuda 1988), the same range in which the observed relative countrate variation is lowest. This behavior is expected in the Comptonizing flow model, which predicts that the countrate oscillations will be a minimum near the pivot energy E_p and that the phase of the oscillations above E_p will differ by 180° from the phase of the oscillations below E_p, if one neglects the phase shifts $\sim(t_{esc}/P_{osc})180°$ caused by the longer escape time of the more highly Comptonized photons (Lamb 1989, 1991). The observations therefore indicate that the pivot energy lies between 4.5 and 8 keV.

As shown in § 3, the pivot energy predicted by the Comptonizing flow model depends primarily on the electron temperature but also depends weakly on the mean optical depth of the flow. If we assume that the mean optical depth is ~ 10, as suggested by preliminary models of normal branch X-ray spectra (see Lamb 1989, 1991), our Comptonization calculations show that the electron temperature in the flow must be between 0.5 and 1.1 keV in order for the pivot energy to lie in the range 4.5–8 keV. However, electron temperatures in the

range 0.5–0.7 keV give predicted countrate variations in the two highest-energy bins shown in Figure 9 that are larger than the observed countrate variations. The Comptonizing flow model is consistent with the countrate variations observed at all energies if the electron temperature in the flow is in the range 0.8–1.1 keV.

This estimate of the electron temperature in the flow is in striking agreement with our best estimate of the Compton temperature of the Cyg X-2 normal branch X-ray spectrum, which we made by extending the spectral fits published by Schulz et al. (1989) to lower X-ray energies and truncating the spectrum at $E_{\rm low}$. For any $E_{\rm low} \lesssim 1$ keV, we find $T_c' \approx 1.0 \pm 0.2$ keV, where the stated uncertainty in T_c' reflects our estimate of the uncertainty in the shape of the X-ray spectrum below 2 keV.

The mean optical depth τ of the Comptonizing flow is only weakly constrained by current measurements of the relative NBO amplitude, since these measurements do not extend to energies high enough to allow a direct determination of $\Delta\tau/\tau$. However, if the high-energy cutoff is at ~ 5 keV when Cyg X-2 is on the normal branch, as reported by Schulz et al. (1989), and this cutoff is produced by Compton degradation of a power-law spectrum from the central corona, as suggested by preliminary spectral modeling (see Lamb 1989, 1991), then the mean optical depth is ~ 10. Time-dependent radiation-hydrocode simulations of the normal branch oscillations also indicate that the mean optical depth of the radial flow is ~ 10 (Fortner, Lamb, & Miller 1989, 1991).

The inferred variation in the optical depth of the Comptonizing flow depends on the electron temperature and the mean optical depth of the flow. For electron temperatures in the range 0.8–1.1 keV and mean optical depths in the range 6–15, the inferred optical depth variation is in the range 0.7–1.6, with the largest variations inferred for the smallest mean optical depths. This accords with equation (2.30), which predicts that the relative NBO amplitude at energies below E_p should be roughly proporational to $T_c \tau \Delta\tau$. Variations of this size in the optical depth of the Comptonizing flow agree with the results of time-dependent simulations of the normal branch oscillations (Fortner, Lamb, & Miller 1989, 1991). For $\tau = 10$ and $T_e = 1$ keV, we find that the rms variation $\Delta\tau \approx 0.9$. Figure 9 shows the relative NBO amplitude predicted by the oscillating Comptonization model for this choice of parameters. The predicted variation is in excellent agreement with the observed NBO amplitude, indicating that the model is successful for this source.

The agreement between the electron temperature predicted by the oscillating Comptonization model and the estimated Compton temperature of the Cyg X-2 X-ray spectrum, when combined with the qualitative agreement between the countrate oscillations predicted by the model and the observed countrate oscillations, provides strong support for the idea that the NBOs observed in Cyg X-2 are caused largely by oscillations in the optical depth of a Comptonizing flow surrounding the central radiation source.

The oscillating Comptonization model predicts that the relative amplitude should asymptotically approach the value $-4(\Delta\tau/\tau)$ at energies well above 10 keV (see eq. [2.34]). Thus, measurements of the relative oscillation amplitude at these energies would provide another check on the validity of the model.

It is difficult to determine the effective radius $r_{\rm Compt}$ of the Comptonizing flow from current measurements of the relative NBO amplitude, because these measurements do not extend to sufficiently low X-ray energies. However, the measurements made at the lowest energies to which the *Ginga* LAC detectors respond, combined with the results of § 3, do provide a rough lower bound on $R_{\rm Compt}$.

First consider the additional node that appears in the relative NBO amplitude when induced scattering is important. Figure 6 shows that if $E_{\rm low} = 0.1$ keV and $s = 0$, which corresponds to an infinite effective radius, this node is at an energy well below 1 keV. If instead $s \gtrsim 10^{-8}(m_e c^2)^2$, which corresponds to an effective radius $r_{\rm Compt} \lesssim 8 \times 10^6$ cm, the node moves to energies greater than ~ 1 keV. The node would move to even higher energies if the spectrum actually turns over just below 1 keV, rather than at 0.1 keV, since photons would then diffuse rapidly to low energies. There is no evidence in the Cyg X-2 data of a second node in the relative NBO amplitude below the node associated with the pivot energy E_p (see Fig. 9), and hence we conclude that the effective radius of the Comptonizing region is $\gtrsim 8 \times 10^6$ cm.

We can obtain another bound on $r_{\rm Compt}$, because the Compton temperature T_c increases with increasing s, all other things being equal (see eq. [2.12]). If the power-law behavior of the Cyg X-2 X-ray spectrum extends to energies as small as 0.1 keV, the bound on the Compton temperature derived from the value of the pivot energy ($T_c \leq 1.1$ keV) implies $s \lesssim 10^{-8}(m_e c^2)^2$ and hence again $r_{\rm Compt} \gtrsim 8 \times 10^6$ cm. If instead the spectrum turns over at a higher energy, the lower bound on $r_{\rm Compt}$ increases. Although these bounds on $r_{\rm Compt}$ are necessarily tentative, they are nevertheless tantalizing.

Finally, it is interesting to ask if the variation in the Cyg X-2 X-ray spectrum during a normal branch quasi-periodic oscillation corresponds to small motions up and down the normal branch, since if this were true it would suggest that the physical process responsible for the NBO is similar to the physical process that causes Cyg X-2 to move up and down the normal branch. Answering this question requires accurate differencing of the X-ray spectra observed at different points on the normal branch. The only spectral fits that are currently available are those of Schulz et al. (1989), which probably do not reproduce the observed spectra accurately enough to answer this question definitively. We note nevertheless that differencing of these spectra suggests that the pivot energy associated with motion along the normal branch is ≈ 3 keV, somewhat lower than the pivot energy indicated by the *Ginga* NBO data. If this difference in pivot energies is real, the spectral changes that cause Cyg X-2 to move down the normal branch probably involve some softening of the emission from the central source as well as Comptonization of this emission by the radial flow.

5. SUMMARY AND CONCLUSIONS

We have investigated further the radiation-hydrodynamic model of NBOs in Z sources. In this model, the NBOs are produced by quasi-periodic oscillations in the optical depth of a radial inflow from the inner part of the accretion disk to a compact central corona surrounding the neutron star magnetosphere. The optical depth oscillations cause oscillating Comptonization of X-rays coming from the central corona.

We have developed a quantitative model of the Comptonizing radial flow that includes the upscattering and diffusion caused by electron thermal motions, the upscattering produced by the convergence of the flow, the downscattering due to electron recoil, and the effects of induced scattering. Using this model, we have investigated the dependence of the NBO amplitude on the shape of the X-ray spectrum coming

from the central corona as well as the temperature and mean optical depth of the radial flow, and its optical depth variation.

We find that the properties of the relative NBO amplitude depend only weakly on the shape of the X-ray spectrum emitted by the central corona, but are sensitive to the properties of the Comptonizing flow, particularly its temperature. As a result, it is possible to test the hypothesis that the NBOs are caused largely by oscillations in the optical depth of a Comptonizing flow, even though we do not yet have a detailed physical model of the central radiation source. Moreover, if the oscillating Comptonization hypothesis is successful, one can infer the properties of the Comptonizing flow with relatively high confidence.

We have shown that one can read off the electron temperature, mean optical depth, and optical depth variation from the basic features of the oscillation amplitude. The detailed shape of the oscillation amplitude as a function of energy then provides a test of the validity of the model. According to the model, the electron temperature inferred from the oscillation amplitude should be similar to the Compton temperature of the observed X-ray spectrum. Thus, the validity of the model can be tested further by comparing these two temperatures.

We have compared the predictions of our Comptonization model with the observed properties of the 6 Hz normal branch spectral oscillations in Cyg X-2, one of the best-studied Z sources. This comparison strongly suggests that these oscillations are indeed produced by oscillations in the optical depth of a Comptonizing flow surrounding a central photon source. We find that the Comptonizing flow model is consistent with the countrate variations at all energies if the electron temperature in the flow is the range 0.8–1.1 keV. This estimate of the electron temperature in the flow is in excellent agreement with our best estimate of the Compton temperature of the Cyg X-2 normal branch X-ray spectrum. The inferred optical depth of the Comptonizing flow is ~ 10 while the inferred variation of the optical depth is ~ 1. Our investigation of the effects of induced scattering on the X-ray spectrum suggests that the effective radius of the Comptonizing flow is $\gtrsim 8 \times 10^6$ cm.

Normal-branch quasi-periodic oscillations that are qualitatively similar to the oscillations seen in Cyg X-2 have been reported in GX 5−1 by G. Hasinger (1989, private communication) and K. Mitsuda (1989). We speculate that these oscillations and the 6 Hz normal branch quasi-periodic oscillations observed in the Z sources generally are due largely to oscillations in the optical depth of a Comptonizing flow that surrounds the central photon source.

We thank Nick Kylafis for stimulating conversations, and Norbert Schulz and Günther Hasinger for helpful discussions of the continuum spectra of Cyg X-2. G. M. is grateful to Kazuhisa Mitsuda and Tadayasu Dotani for providing their QPO amplitude data in convenient tabular form, for valuable conversations about *Ginga* QPO observations, and for hospitality while he was visting the Institute for Space and Astronautical Science in Japan. This work was supported by NASA grant NAGW 1583 and NSF grants PHY 86-00377 and PHY 91-00283 at the University of Illinois, and by the US Department of Energy at Los Alamos.

APPENDIX A

ESCAPE PROBABILITY AT LOW OPTICAL DEPTHS

The prescription (2.4) for the escape probability may be modified to crudely account for photons which escape without scattering by using

$$P(t) = (1 - e^{-\tau})(1 - e^{-t/t_{\rm esc}})^2 + e^{-\tau}\Theta(t/t_{\rm esc}) , \tag{A1}$$

where Θ is the unit step function ($\Theta[x] = 1$ if $x \geq 0$, $\Theta[x] = 0$ otherwise).

APPENDIX B

ASYMPTOTIC PHOTON DISTRIBUTIONS

Suppose that the photon distribution evolves in time according to the modified Kompaneets equation (2.8) *with the electron temperature T_e held fixed.* As $t \to \infty$, the distribution will approach the asymptotic distribution

$$f_\infty(E) = \frac{(E/m_e c^2)^{(a/b)-2} e^{-E/(bm_e c^2)}}{c_0 + (s/b)\displaystyle\int_0^{E/m_e c^2} z^{(a/b)-4} e^{-z/b}\, dz} (m_e c^2)^{-1} , \tag{B1}$$

where

$$a \equiv \frac{t_c}{t_u} + 4\frac{k_B T_e}{m_e c^2} , \tag{B2}$$

$$b \equiv \frac{k_B T_e}{m_e c^2} , \tag{B3}$$

and the constant c_0 is chosen to ensure that f_∞ is correctly normalized, that is

$$\int_0^\infty f_\infty(E)\,dE = 1\,. \tag{B5}$$

The distribution $f_\infty(E)$ is stationary ($D[f_\infty] = 0$) and satisfies zero-flux boundary conditions at $E \to 0$ and $E \to \infty$.

When induced scattering and upscattering by the converging flow are unimportant ($s = 0$ and $[t_c/t_u] = 0$), the distribution (B1) becomes the Wien spectrum,

$$f_{\rm Wien}(E) = \frac{1}{2k_B T_e}\left(\frac{E}{k_B T_e}\right)^2 \exp\left(-E/k_B T_e\right)\,. \tag{B6}$$

In the Comptonization model considered in this paper, the converging flow causes systematic upscattering of the photons while the interaction of the electrons with the photons keeps the electron temperature close to the Compton temperature. The asymptotic limit described above then cannot be obtained, since the upscattering produces a distribution with an ever-increasing Compton temperature and hence the photon distribution continues to evolve indefinitely.

REFERENCES

Alpar, M. A., & Shaham, J. 1985, Nature, 316, 239
Blandford, R. D., & Payne, D. G. 1981, MNRAS, 194, 1033
Colpi, M. 1988, ApJ, 326, 223
Fortner, B., Lamb, F. K., & Miller, G. S. 1989, Nature 342, 775
———. 1991, ApJ, submitted
Hasinger, G., & van der Klis, M. 1989, A&A, 225, 76
Katz, J. I. 1987, High Energy Astrophysics (Menlo Park, CA: Addison Wesley)
Katz, J. I. 1976, ApJ, 206, 910
Lamb, F. K. 1989, in Proc. 23rd ESLAB Symposium on X-ray Astronomy (Bologna: ESA SP-296), 215
———. 1991, ApJ, submitted
Lamb, F. K., Shibazaki, N., Alpar, M. A., & Shaham, J. 1985, Nature, 317, 681
Lewin, W. H. G., van Paradijs, J., & van der Klis, M. 1988, Spa. Sci. Rev., 46, 273
Miller, G. S. 1990, ApJ, 356, 572
Mitsuda, K. 1988, in Physics of Neutron Stars and Black Holes, ed. Y. Tanaka (Tokyo: Universal Academy Press), 117
Mitsuda, K. 1989, in Proc. 23rd ESLAB Symposium on X-ray Astronomy (Bologna: ESA SP-296), 197
Park, M.-G., & Miller, G. S. 1991, ApJ, 371, 708
Ponman, T. J., Foster, A. J., & Ross, R. R. 1990, MNRAS, 246, 287
Press, W. H., Flannery, B. P., Teukolsky, S. A., & Vetterling, W. T. 1986, Numerical Recipes (Cambridge: Cambridge Univ. Press)
Rybicki, G. B., & Lightman, A. P. 1979, Radiative Processes in Astrophysics (New York: Wiley), 195
Schulz, N. S., Hasinger, G., & Trümper, J. 1989, A&A, 225, 48
Shapiro, S. L., Lightman, A. P., & Eardley, D. M. 1976, ApJ, 204, 187
Shibazaki, N., & Lamb, F. K. 1987, ApJ, 316, 767
Sunyaev, R. A., & Titarchuk, L. G. 1980, A&A, 86, 121
van der Klis, M. 1989, ARAA, 27, 517
White, N. E., Stella, L., & Parmar, A. N. 1988, ApJ, 324, 363